Chapter 6
Recent Applications of Number-Theoretic Sequences in Audio and Acoustics

Ning Xiang, Bosun Xie, and Trevor J. Cox

Abstract Manfred R. Schroeder made influential contributions to acoustics by applying number theory. He introduced number-theory sequences in room impulse response measurements, applied number-theoretical sequences to shape wall surfaces for diffuse sound reflections. Another area Manfred Schroeder made broad impact is invention of an artificial reverberator using all-pass transfer-function properties to create colorless reverberation using a simple algorithm. Vast research activities and engineering developments over past decades have extended Schroeder's work involving artificial reverberators, artificial stereo and applications of maximum-length sequences. This chapter briefs a number of recent applications of maximum-length and quadratic-residue sequences, such as simultaneous dual/multiple sources measurements in acoustical tomography, in artificial pseudo-binaural reverberation, in decorrelation for spatial audio signals, and room acoustic diffuser design.

6.1 Introduction

In 1961, Manfred R. Schroeder, along with Ben Logan [1, 2] invented an artificial reverberator using all-pass transfer-function properties while having an exponentially decaying impulse response, thereby creating colorless reverberation using a simple algorithm. It has been widely accepted both in analog and digital audio devices for processing audio signals. One can now find colorless reverberators and artificial stereo, including simulations of virtual sound sources and auditory

N. Xiang (✉)
Graduate Program in Architectural Acoustics, School of Architecture, Rensselaer Polytechnic Institute, Troy, NY 12180, USA
e-mail: xiangn@rpi.edu

N. Xiang and G.M. Sessler (eds.), *Acoustics, Information, and Communication*, Modern Acoustics and Signal Processing, DOI 10.1007/978-3-319-05660-9_6,

environments in various stereophonic and surround sound reproduction formats, in practically all electronic music instruments (See Schroeder's Memoirs in Part II).

In the 1970s, Manfred Schroeder made another influential contribution to acoustics with the introduction of number-theory sequences, applying bipolar, binary maximum-length sequences (MLSs) to applications such as shaping wall surfaces for diffuse sound reflections [3], and acoustics system identification to enable room impulse response measurements based on correlation techniques [4]. Extending the wall surface work to exploit nonbinary sequences, led to Schroeder devising the quadratic residue diffuser [5] and other designs widely used in studios and performance spaces to improve acoustics [6] (see also Chap. 9).

Vast research activities and engineering developments over past decades have extended Schroeder's work involving artificial reverberators, artificial stereo and applications of MLSs. This chapter is dedicated to the memory of Manfred Robert Schroeder in briefing a number of recent applications of maximum-length and quadratic residue sequences, such as simultaneous dual/multiple sources measurements in acoustical tomography, in artificial pseudo-binaural reverberation, in decorrelation for spatial audio signals, and room acoustic diffuser design.

6.2 Properties of Maximum-Length Related Sequences

MLSs, also termed pseudorandom sequences/noises, offer excellent pseudorandom properties. Therefore, they are used in communication, acoustics, and many other relevant applications. They possess properties similar to those of random noise, but are periodically deterministic and have a strict time structure within their periods. In the following, a brief review of some basic properties pertaining to acoustic applications is given. Detailed description and definitions can be found in [7–9]. In particular, Xiang [9] has most recently summarized these properties succinctly.

An n-stage linear shift-register device with proper feedback taps can generate periodic binary MLSs $\{a_i\}$ with $a_i \in (0, 1)$. Binary MLSs can also be generated numerically using a simple recurrence in the digital domain

$$a_i = \sum_{k=1}^{n} c_k a_{i-k}, \quad 0 \le i < L, \tag{6.1}$$

with $c_k \in (0, 1)$ and $c_0 = c_n = 1$, where the summation and indices are calculated, *modulo* 2 and the positive integer n is said to be the *degree* of the linear feedback registers or of the corresponding MLS. Both analog generation using linear feedback registers and numerical generation using the linear recurrence are subject to a nonzero *initial state* $\{a_{-n}, a_{-n+1}, a_{-n+2}, \ldots a_{-2}, a_{-1}\}$ denoted as $\{\overleftarrow{a}_i\} \neq \{0\}$. The proper feedbacks are expressed by feedback coefficients $c_k \in (0, 1)$; when resulting in a periodic sequence of length $L = 2^n - 1$, the sequence arrives at its maximum possible length, therefore, termed MLS. Under

this MLS condition, the proper set of feedback coefficients can also be expressed in polynomial form, $f(x) = \sum_{k=0}^{n} c_k x^k$, termed the *primitive polynomial*. One primitive polynomial given degree n corresponds uniquely to one MLS. The feedback coefficients c_k and the binary sequence element a_i are defined over Galois field GF(2) while the sequence $\{a_i\}$ is defined over Galois field $GF(2^n)$. The underlying mathematical calculus is a substantial subject of number theory [7].

Among a number of number-theoretic properties, the most important property of MLS is that the normalized periodic autocorrelation function of a bipolar MLS within one period is a two-valued function [8]

$$\phi(i) = \frac{L+1}{L}\delta(i) - \frac{1}{L}. \tag{6.2}$$

With large enough period length $L = 2^n - 1$, the periodic autocorrelation function approximates the *unit sample sequence* $\phi(i) \approx \delta(i)$. Therefore the power spectrum of any MLS is flat, expect for a "dip" at zero-frequency.

An MLS $\{b_i\}$ can always be derived from a given one $\{a_i\}$ in terms of a circular phase shift such that $b_i = a_{i+\tau}$ so that an invariant decimation $b_i = b_{2i}$ can be satisfied. Here all the indices are calculated modulo L. This specific MLS $\{b_i\}$ is designated as *characteristic* MLS and *self-similar* MLS [9]. This invariant decimation holds only for characteristic MLSs with decimation factors of 2^m with m being a positive integer [9]. There exists a unique characteristic MLS for any given primitive polynomial and a unique initial state $\{\overleftarrow{a}_i\}$ of the shift register to generate it. An algorithm deriving the required initial state $\{\overleftarrow{a}_i\}$ given the primitive polynomial for generating the characteristic MLS has recently been described by Xiang [10]. The characteristic MLSs with the invariant decimation are of practical significance, they are also relevant to the following applications.

Furthermore, *a variant decimation* is also of practical significance. When the decimation factor d is properly chosen, the decimation will lead to a pair of MLSs $(\{a_i\}, \{b_i\})$ with $\{b_i\} = \{a_{di}\}$, whose periodic cross-correlation function (PCCF) is of clearly lower value than the peak of the periodic autocorrelation function of either sequence. In this context, all the indices are calculated modulo L. One of the straightforward variant-decimation factors is $d = L - 1$. This decimation $\{b_i\} = \{a_{(L-1)i}\} = \{a_{-i}\}$ simply indicates that a time reversal of MLS $\{a_i\}$ always leads to another MLS $\{b_i\}$. This pair of MLSs $(\{a_i\}, \{b_i\})$ derived from decimating $\{a_i\}$ using factor $d = L - 1$ or equivalently from time reversing $\{a_i\}$ is termed reciprocal MLSs due to the fact that their corresponding primitive polynomials are reciprocal to each other [10]. The most relevant correlation properties pertaining to the applications described in this chapter are that one can find MLS pairs or sets of sequences such that the PCCFs between them are of lower values, and the absolute bounds of these low values are deterministically predictable. For example, the bound value of the reciprocal MLS pair of degree n has been reported [8, 11]

$$l_r(n) = \frac{2^{(n+2)/2} - 1}{2^n - 1}. \tag{6.3}$$

For MLSs whose degrees are not a multiple of 4, some decimation factors are of the form $d = 2^k + 1$ or $d = 2^{2k} - 2^k + 1$, where k is chosen such that $n/\gcd(n, k)$ is odd, with gcd(,) being the greatest common divider. A decimation using these factors leads to an MLS pair $(\{a_i\}, \{b_i\})$, with $\{b_i\} = \{a_{di}\}$. For MLSs whose degrees are a multiple of 4, a decimation factor $d = 2^{(n+2)/2} - 1$ leads to a MLS pair. The cross-correlation between the original MLS $\{a_i\}$, and the decimated one $\{b_i\}$ results in small values bounded [8] by

$$l_p(n) = \frac{2^{\lfloor (n+2)/2 \rfloor} - 1}{2^n - 1}, \tag{6.4}$$

where $\lfloor \alpha \rfloor$ denotes the integer part of the real number α.

Besides the reciprocal MLS pairs, this chapter will refer to MLS pairs derived from above-mentioned decimation factors with low-valued PCCFs as *preferred MLS pairs* (see Xiang [8] for a detailed summary). In addition, one can derive a large number of sequences by combining the preferred or reciprocal MLS pairs $(\{a_i\}, \{b_i\})$, as $G_\tau(i) = a_i \oplus b_{i+\tau}$ with $\oplus$ denoting addition modulo 2, so-called Gold sequences $\{G_\tau(i)\}$, whose correlation bound values between each other are the same as those of either preferred MLS pairs or reciprocal pairs [8]. Similarly a decimation from an MLS $\{a_i\}$ of even-numbered degree with a decimation factor $d = 2^{n/2} + 1$ leads to a pair $(\{a_i\}, \{e_i\})$, with $e_i = a_{di}$. The combination $K_\tau(i) = a_i \oplus e_{i+\tau}$ leads to a binary Kasami sequence $\{K_\tau(i)\}$, and their low-valued PCCFs represent even lower bounds,

$$l_K(n) = \frac{2^{n/2} + 1}{2^n - 1}, \tag{6.5}$$

approximately half of those of preferred pairs and Gold sequences.

Figure 6.1 illustrates the bounds of the PCCF of preferred pair, reciprocal pairs, and Kasami sequences. Gold sequences have the same bound values as those of preferred pairs and reciprocal pairs for even-numbered degrees. The preferred pairs possess approx. 3 dB lower bound values than those of reciprocal pairs for odd-numbered degrees. And the bound values of Kasami sequences, existing only for even-numbered degrees, are as $6 \sim$ dB lower than those of the others. Figure 6.2 shows auto- and cross-correlation functions of Kasami sequences of degree 14 to illustrate the excellent correlation properties of MLS-related sequences.

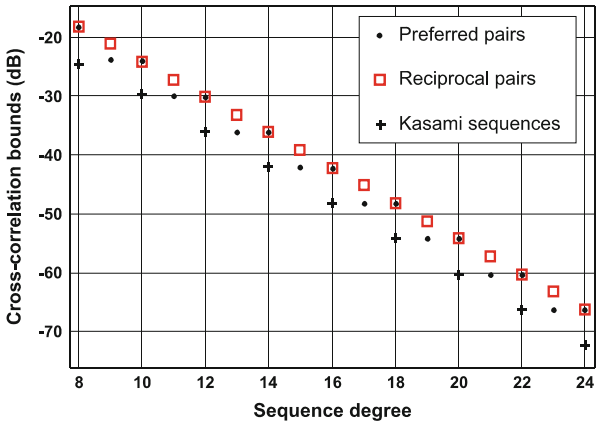

Fig. 6.1 Bound values of the cross-correlation functions of preferred, reciprocal MLS pairs and of Kasami sequences. The bound values are expressed in dB relative to the peak value of their normalized autocorrelation function [11]. [Reproduced from Xiang, N., Daigle, J. N., and Kleiner, M.: Simultaneous acoustic channel measurement via maximal-length-related sequences, *J. Acoust. Soc. Am.*, 117, 2005, pp. 1889–1894. Copyright 2005, Acoustical Society of America.]

6.3 Acoustical Measurements Using Simultaneous Sound Sources

Recent research in outdoor sound propagation for acoustic atmospheric tomography [12] calls for a critical measurement exploiting these correlation properties of MLSs and related coded signals. In tomographical applications, a number of sound sources have to be excited at the same time, within the same frequency range. This simultaneous multiple acoustic source measurement (SMASM) can be used in acoustic delay-time tomography to investigate temperature distributions and wind profiles near the ground surface in outdoor environments. With simultaneous excitations of multiple sound sources and one or multiple sound receivers, the SMASM considers the acoustic system under test as a linear time-invariant multiple-inputs and multiple-outputs (MIMO) system, at least approximately during the excitation period. Using the excellent correlation properties of the coded signals (sequences) briefly discussed above, a large number of coded signals can be straightforwardly derived for the SMASM technique.

Figure 6.3 illustrates a SMASM scheme, where the vector $\mathbf{s} = [s_1, \ldots s_n]^T$ stands for the multiple coded signals used as system excitations, and $\mathbf{r} = [r_1, \ldots r_p]^T$ denotes the system's responses to these excitations, with $[,]^T$ standing for matrix transpose; n is the number of simultaneous sources, while p is the number of receivers.

With properly designed excitations, the system identification task is to determine the impulse response matrix $\mathbf{h} = [h_{ij}]$ for $1 \leq i \leq p$, $1 \leq j \leq n$, determined by

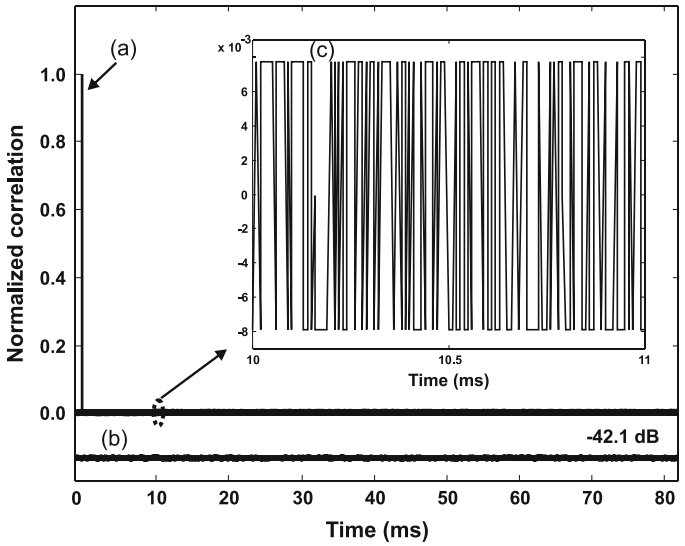

Fig. 6.2 Normalized correlation functions of 14-degree Kasami sequences [9]. (a) Periodic autocorrelation function (PACF) of individual sequences. (b) Periodic cross-correlation function (PCCF) between two Kasami sequences (shifted downwards beneath the autocorrelation function for a convenient comparison). The peak value of the PCCF is 42.1 dB lower than that of the delta-like PACF. (c) Magnified presentation of a segment from (a). Their peak values in the side-lobe of the PACF are the same as those of the PCCF in (b). [Reproduced from Xiang, N., Daigle, J. N., and Kleiner, M.: Simultaneous acoustic channel measurement via maximal-length-related sequences, *J. Acoust. Soc. Am.*, 117, 2005, pp. 1889–1894. Copyright 2005, Acoustical Society of America.]

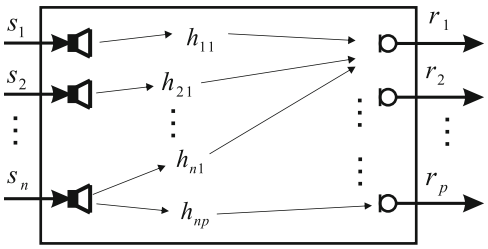

Fig. 6.3 An acoustical linear time-invariant system under investigation with n number of sound sources and p number of sound receivers. An $p \times n$ impulse response matrix $\mathbf{h}$ describes the entire system under investigation

$$\mathbf{h} \approx \mathbf{r} \otimes \mathbf{s}^T, \tag{6.6}$$

with $\otimes$ denoting periodic cross-correlation and the correlation properties discussed above leading to this concise form [11]. The physical meaning of Eq. (6.6) is that the cross-correlation between the receiver (column) vector $\mathbf{r} = [r_1, \ldots r_p]^T$ and the source (row) vector $\mathbf{s}^T = [s_1, \ldots s_n]$ approximately results in the channel impulse

response matrix **h**. The approximation is due to the fact that the cross-correlation functions among individual source signals in the form of coded sequences (Kasami sequences, preferred and reciprocal MLS pairs) are of finite low-values rather than zeros. In calculating the individual cross-correlations as expressed in Eq. (6.6), particularly for $n > 2$, a specialized algorithm [13] can be used for efficient calculations. In the case of $n = 2$, reciprocal MLS pairs can be exploited with a dedicated fast MLS transform algorithm recently published by Xiang and Schroeder [10].

6.4 Artificial Reverberations Using Reciprocal MLS Pairs and Related Sequences

Following Schroeder [1, 2], there have been many developments of all-pass filter type artificial reverberators. The most recent overviews on all-pass-filter artificial reverberators can be found in [14, 15]. Another line of development is reverberators using finite-impulse-response (FIR) filters, probably due to Moorer [16]. He proposed the use of exponentially decaying random noise for the late part of room impulse responses, so that when convolved with anechoic sound materials, artificial reverberation with a desirable degree of reverberance is created. With the rapid advent of digital audio processing on personal-computer and DSP platforms, FIR filtering via linear convolutions have reached multiples of real-time speed at low cost, so that even a large number of multiple audio channels can be filtered in real-time with sufficiently long FIR-filter coefficients (room impulse responses). FIR-filtering algorithms have also emerged that ensure sufficiently short latency for long room impulse responses [17].

There is a need for rendering the FIR-filter-based artificial reverberations binaurally, such as in binaural room-acoustic simulations [18], where the tails of binaural room impulse responses (see Fig. 6.4) are replaced by exponentially decaying random noise. The decay rates (reverberation times) are determined via statistical room-acoustic principles. Alternately, other room-acoustic information is first extracted from the early part of detailed room-acoustic simulations, such as ray-tracing, image-source approaches, or hybrid approaches [18]. Such schemes have recently been used for psychoacoustics studies investigating speech intelligibility, as well as perceptual aspects of acoustically coupled-volume systems [19].

In principle, an artificial reverberation for a binaural rendering can be achieved with a spatial envelopment, so-called *listening envelopment* when the two random-noise late reverberation tails are incoherent. This avoids using geometrical room-acoustic simulation (e.g., ray-tracing) to simulate the late reverberation tails, saving extremely time-consuming processing given the current technology in numerical simulations. Reciprocal MLS pairs have been used [19, 20] for this purpose, since the cross-correlation between pairs, given the MLS degree, is of low-value (see Fig. 6.2). The intriguing aspect of using MLS pairs, in contrast with other methods

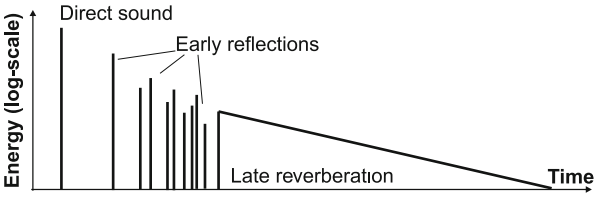

Fig. 6.4 Conceptual echogram containing the direct sound, early reflections, and the late reverberation tail

used in previous work [18] are that MLS pairs (and their related coded sequences) possess deterministically predictable, low values of cross-correlation. Hardly any other random noise signals can be found as low as these, Kasami sequences being the lowest. Lower values correspond to a high degree of enveloping spaciousness in the reverberance. In addition to the highest achievable degrees of spatial envelopment, one can use mix-networks [20] to control the cross-correlation values of the mixed MLS pairs for binaural channels, so that the degree of spatial envelopment can also be adjusted. This is of practical value, since different enclosure conditions will provide different spaciousness, in addition to the reverberance. As recent psychoacoustical investigations [21, 22] have demonstrated, simply shaping the decaying slopes of random noise in the late reverberation tails for achieving artificial reverberations using FIR-filtering technique is not sufficient in terms of naturalness and spatial envelopment of the artificial reverberation. Our recent work [21, 22] adjusts the decay slope (for controlled reverberance) in individual octave/third-octave bands. For each band, the target-reverberation time shapes the exponentially decaying envelope of the reciprocal MLS pair. In addition, interaural decorrelation coefficients which are complimentary to interaural cross-correlation coefficients (IACC) of the binaural reverberation tails

$$\text{IADC} = 1 - \text{IACC}, \tag{6.7}$$

in the individual bands also need to be adjusted accordingly in order to achieve targeted degrees of spatial envelopment. Adjusting only the decay slopes and the interaural decorrelation coefficients so that they are similar to those often observed in experimentally measured binaural room impulse responses creates natural sounding, artificial reverberance with the desired (or targeted) spatial envelopment. Figure 6.5 illustrates the procedure of the binaural artificial reverberation with controllable spatial envelopment and reverberance. A reciprocal MLS pair is first octave-band filtered. Two channels of band-pass filtered pseudorandom noise are mixed with an attenuation factor α_k with $0 \leq \alpha_k \leq 1$ and k being the octave-band index running from 63 Hz to 8 kHz at each octave-band step.

In Fig. 6.5 between "A" and "B" the two channels of the band-pass filtered, reciprocal MLS-pair are mixed to obtain the desired "interaural decorrelation." The band-pass filtered pseudorandom noise is then multiplied by an exponentially decaying function $E = \exp(-6.9 \cdot t/T_k)$, with the desired reverberation time T_k within octave band k. For broadband resulting "binaural" reverberation tails (late portion of room impulse responses)

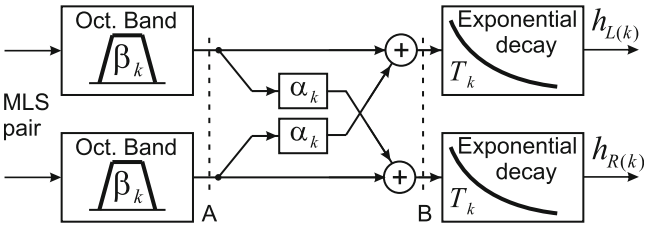

Fig. 6.5 Generation of single-band "binaural" reverberation tails with controllable interaural decorrelation coefficients and the reverberation times within octave band (k)

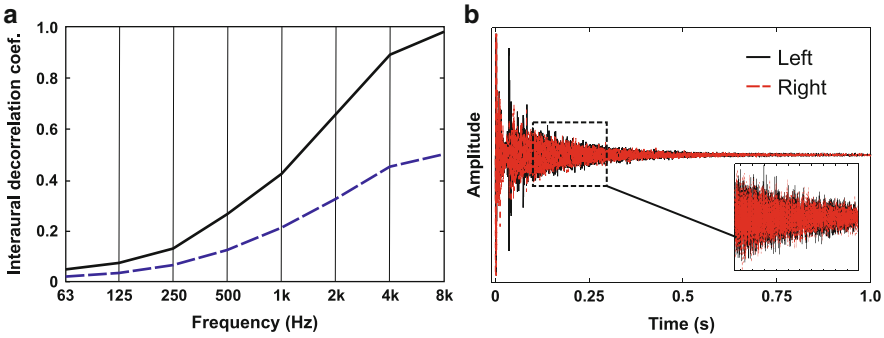

Fig. 6.6 Spatial profiles and the reverberation tails. (a) Two spatial profiles (large spaciousness, middle spaciousness) adjusted for two different degrees of listening envelopment. Interaural decorrelation is defined as 1 – IACC. (b) "Binaural" reverberation tails, properly scaled in terms of amplitude, it will be appended to the early portion of a pair of "binaural room impulse responses at time instance at 90 ms

$$h_{\mathrm{L,R}} = \sum_{k=1}^{M} h_{\mathrm{L,R}(k)}, \tag{6.8}$$

with $k = 1$ for octave band 63 Hz, $k = M$ for octave band 8 kHz, other k values correspond octave bands between 125 Hz and 4 kHz. In order to create naturally sounding, enveloping reverberance, in addition to the desired reverberation time profile, the interaural decorrelation profile also has to be adjusted. Figure 6.6a illustrates two different profiles of interaural decorrelation obtained using Fig. 6.5, inspired from analysis of experimentally measured binaural room impulse responses in existing real concert halls. Figure 6.6b illustrates one (binaural) pair of late-portion artificial "reverberation tails."

Advantages of this artificial enveloping reverberation scheme using reciprocal MLS-pairs are

- MLSs of degree 16–19 with a length between $2^{16} - 1$ and $2^{19} - 1$ are typical lengths used for the artificial reverberation application. At standard audio sampling frequency, the reciprocal MLS pairs are easily generated, and they

provide sufficient reverberation density when sampled using standard audio sampling frequency.
- Spectral flatness of each individual MLS ensures a colorless reverberance.
- Low cross-correlation values of reciprocal MLS pairs (see Fig. 6.2) ensure a high degree of listener envelopment. Reduced degrees of listener envelopment can be straightforwardly achieved using a mixing network [20].

6.5 Decorrelation of Audio Signals Using Reciprocal MLS Pairs [23]

Audio signal decorrelation is a technique that creates two or more replicas of an input signal, which have different waveforms but are perceived similarly to the original signals in most aspects except in some spatial auditory effects [24]. This is applicable to a variety of spatial audio processing effects, such as broadening the auditory source width, enhancing the listener envelopment in surround sound reproduction, and the externalization of auditory events in headphone representation, among others.

In order to create decorrelated audio signals without altering perceived timbre, decorrelation processing should change the signal waveform but leave the magnitude or power spectra of signals intact. A straightforward method is to filter the input signal with a pair of all-pass digital filters with unit magnitude and random phase responses ranging from $-180°$ to $180°$ at every discrete frequency. However, the degree of decorrelation resulting from this method is uncontrollable and unrepeatable.

As stated above, bipolar MLSs are pseudorandom sequences with deterministic and periodic structures, but possess characteristics similar to random noise. In particular, the favorable characteristics of nearly uniform power spectra and deterministic, low-valued cross-correlation functions between each reciprocal MLS pair make it an excellent candidate for the design of all-pass digital filters for audio signal decorrelation. In addition, taking advantage of the deterministic and periodic characteristics of MLS, the design of MLS-based decorrelation filters is controllable and repeatable. This is the advantage of MLS-based decorrelation filters over conventional all-pass filter with random phase. We can also use Kasami sequences or other coded pairs for the decorrelation algorithm, but reciprocal MLS pairs are easier to generate.

The design steps of reciprocal MLS decorrelation filters are outlined as follows:

1. Create a pair of n-degree or $L = 2^n - 1$ points reciprocal bipolar MLSs $\{a_i\} = \{a_0, a_1, \ldots a_{L-2}, a_{L-1}\}$ and $\{b_i\} = \{b_0, b_1, \ldots b_{L-2}, b_{L-1}\} = \{a_{L-1}, a_{L-2}, \ldots a_1, a_0\}$.
2. Sequences $\{a_i\}$ and $\{b_i\}$ are respectively used as the coefficients of a decorrelation FIR-filters pair.

As shown in Eq. (6.3) and Fig. 6.1, the bounds of the normalized periodic cross-correlation value of a reciprocal MLS pair, and thereby that of the reciprocal MLS-based filter coefficients, decreases with increasing degree or length of the MLS. A high degree or long length leads to nearly zero cross-correlation between the filter coefficients. The normalized cross-correlation between two filtered output signals is related to the normalized cross-correlation of filter coefficients and normalized autocorrelation $\Phi_0(n)$ of the input signal by:

$$\Phi_{\text{out}} = \Phi_{ab}(n) * \Phi_0(n), \tag{6.9}$$

where $\Phi_{ab}(n)$ is the normalized PCCF of the reciprocal MLS pair. Therefore, the lower the values of normalized cross-correlation between filter coefficients, the more obvious the decorrelation effect will be. For a better decorrelation effect, a pair of high degree or long length reciprocal MLS filters is preferred. This makes design of real-time devices complicated, however. In implementing real-time devices, the specialized convolution algorithm discussed in Daigle and Xiang is of highly practical significance [25]. Moreover, filters with excessive length may distort the transient properties of signals. In practice, the length of reciprocal MLS filters is selected as a compromise between decorrelation effect and simplicity.

Because the perceived effect of decorrelation is greater for frequencies below 1 kHz than for high frequency above 3 kHz, the perceived performance of decorrelation filters at a given length can be optimized or improved by properly adjusting the filter coefficients. In fact, a cyclic time shift of inverse-order MLS $\{a_{L-1}, a_{L-2}, \ldots a_1, a_0\}$ yields L new sequences $\{a_0, a_{L-1}, a_{L-2}, \ldots a_1)$, $\{a_1, a_0, a_{L-1}, a_{L-2}, \ldots a_2\}$, and so on. The cyclic time shift of an inverse-order MLS is equivalent to adjusting its phase characteristics. The original sequence $\{a_0, a_1, \ldots a_{L-2}, a_{L-1}\}$ and each of these time-shifted inverse-order MLS exhibit auto- and cross-correlation characters similar to those in Eq. (6.3) and Fig. 6.1. We can select the one from these time-shifted MLSs that makes the cross-correlation of filters output lowest for low-pass input signal (such as below 1.5 kHz).

Similar to the case of artificial reverberation, a pair of output signals with controllable but higher values of cross-correlation can be approximately obtained by an appropriate mixture of the reciprocal MLS pair.

The algorithm of reciprocal MLS-based audio signal decorrelation is applicable to broadening or controlling the auditory source width (ASW) in spatial sound reproduction. The ASW is an important attribute of hall spatial auditory perception and closely related to early lateral reflections in the hall [26]. The early IACC, which is derived from the interaural cross-correlation within the first 80 ms, can be used as an objective index to evaluate ASW. In stereophonic or multichannel surround reproduction, the cross-correlation between/among the loudspeaker signals can also be used to evaluate the degree of the decorrelation effect. Taking conventional stereophonic reproduction as an example, results from psychoacoustic experiments show that a pair of 2,047-point reciprocal MLS filters (at 44.1 kHz sampling frequency) yields a relatively natural decorrelation effect in terms of left-right symmetry of broadened auditory events as well as less timbre coloration.

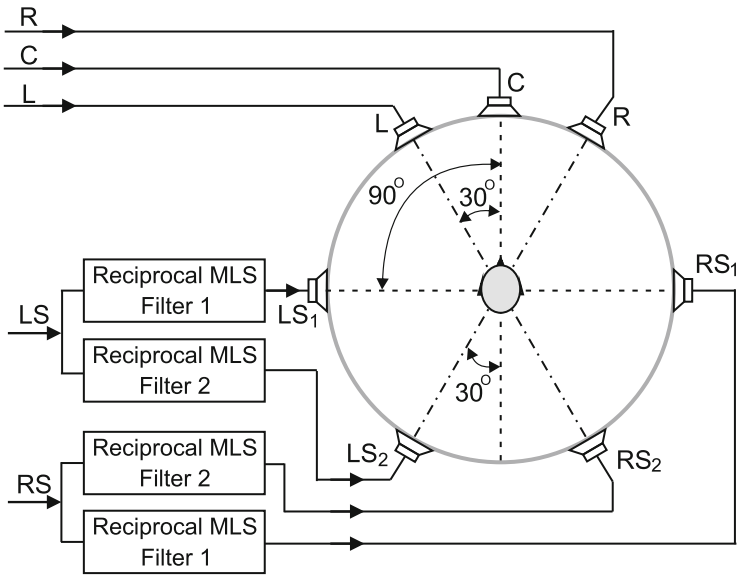

Fig. 6.7 Block diagram of converting 5.1 channel surround sound signals to 7.1 channel surround sound signals

The perceived performance of 511-point filters can be improved using the optimizing scheme mentioned above so that it is perceptually better than the original 1,023-point filters.

Another application of the algorithm of reciprocal MLS-based audio signal decorrelation is enhancing the listener envelopment in surround sound reproduction. It is well known that reproducing decorrelated signals via a series of surround loudspeakers results in the experience of better listener envelopment. An example is converting the 5.1 channel surround sound (music) signals to 7.1 channel reproduction. Figure 6.7 shows the block diagram of such an application. There are five independent full audio bandwidth channels in a 5.1-channel surround sound system, including left (L), center (C), right (R), left-surround (LS), and right-surround (RS), plus an optional low frequency effect channel (called .1 channel, which has been omitted in the figure). In the figure, the original L, C, and R signals are directly reproduced by three corresponding loudspeakers. The original LS and RS signals are filtered by two pairs of reciprocal MLS filters to yield four decorrelated surround signals LS_1, LS_2, LS_3, and LS_4, respectively, and then reproduced by four surround loudspeakers. The two reciprocal MLS pairs are derived from one pair of preferred MLSs. The length of reciprocal MLS filters is 511 points at a 48-kHz sampling frequency, and the optimizing scheme has been incorporated in the filter design. Here, a left-right symmetric decorrelation processing is adopted. That is, the reciprocal MLS filter 1 for signal LS is identical to that for signal RS, and so is the reciprocal MLS filter 2. For two pairs of resultant signals, LS_1 and RS_1 as well as LS_2 and RS_2, when the original signals LS and RS

Fig. 6.8 Gateway Mastering, Portland, ME showing a fractal diffusing rear wall (Diffractal®). (Photo courtesy of Gateway Mastering + DVD)

are decorrelated, the four signals are also decorrelated. While original LS and RS are correlated to each other, the signals within each pair are correlated, and the signals among different pairs are decorrelated. A preliminary subjective experiment shows that the algorithm of reciprocal MLS filter-based decorrelation improves listener envelopment in surround reproduction.

6.6 Diffuser Sequences

Figure 6.8 shows a diffuser applied to the rear wall of a studio, a fractal design which exploited the devices invented by Schroeder in the 1970s. Schroeder originally devised slatted wall surfaces based on MLSs [3], but these devices only operate across about an octave centered around the design frequency. Consequently, Schroeder sought out nonbinary number sequences such as the quadratic residue and primitive root sequences to form diffusers that had wells with many different depths that then operate over a wider bandwidth.

A quadratic residue sequence a_i is given by:

$$a_i = i^2 \bmod N; \quad 0 \leq i < N \tag{6.10}$$

where mod indicates the least nonnegative remainder; N is the number generator that must be an odd prime number and is also the number of wells per period. For example, one period of an $N = 7$ sequence is {0,1,4,2,2,4,1}.

For room diffusers, it is a complex exponential R_i incorporating the sequence that is crucial to how the structure reflects sound:

$$R_i = \exp\left(\frac{2\pi j a_i}{N}\right) \tag{6.11}$$

where j is $\sqrt{-1}$. Schroeder noted that R_i had an "astounding property" [5]. He was referring to the fact that the magnitude of the discrete Fourier Transform was constant and consequently the periodic autocorrelation function is the unit sample sequence.

The diffuser shown in Fig. 6.8 causes scattering in the horizontal plane. To diffuse sound vertically requires two-dimensional number sequences. To do this for a quadratic residue diffuser requires two number sequences, one for the horizontal (x-direction), one for the vertical (z-direction). Then the z-sequence is used to amplitude modulate the x sequence. For a quadratic residue sequence, this can be expressed as [5]:

$$a_{i,k} = \left(i^2 + k^2\right) \bmod N; \quad 0 \le i < N; \;\; 0 \le k < N \tag{6.12}$$

where i and k are the integers that index the sequence in the x and z direction respectively.

Another common method for making multidimensional phase grating diffusers is to use the Chinese remainder theorem [27]. This folds a one-dimensional sequence of length $N \cdot M$ into a two-dimensional array of size $N \times M$ while preserving the ideal autocorrelation and Fourier properties of the one-dimensional sequence. To use this method N and M must be co-prime. By co-prime, it is meant that the only common factor for the two numbers is 1. A quadratic residue sequence cannot be folded using the Chinese remainder theorem because it has a prime number of elements, and so an alternative sequence is needed, and the primitive root sequence is one possibility.

A primitive root sequence a_i is defined as:

$$a_i = r^i \bmod N; \quad 1 \le i < N \tag{6.13}$$

where N is an odd prime, r is the primitive root of N, and the sequence has $N-1$ elements per period. A primitive root is an integer that yields a sequence a_i for $i = 1$, 2, ... $N-1$ that are all unique. For example, $N = 13$ has a primitive root of 2, so $a_i = \{2,4,8,3,6,12,11,9,5,10,7,1\}$, which generates every integer from 1 to $N-1$. Primitive roots can be found by a process of trial and error, alternatively, tables can be found in texts such as [28]. The autocorrelation of the primitive root sequence placed in an exponential using Eq. (6.11) is a two-valued function.

Consider taking the length 12 primitive root sequence and wrapping it into a 3×4 array. The one-dimensional sequence is written down the diagonal of the array, and as it is periodic, every time the edge of the array is reached, the position is folded back into the base period. The process is illustrated in Fig. 6.9.

a_i mod 3 \ a_i mod 4				
	2			3
		4		
			8	

a_i mod 3 \ a_i mod 4				
	2	10	11	3
	6	4	7	9
	5	12	8	1

Fig. 6.9 *Top*: The first four elements of the length 12 primitive root sequence {2,4,8,3,6,12,11,9,5,10,7,1} placed in a 4×3 array using the Chinese Remainder Theorem. *Bottom*: the final complete table for one period

This sequence folding technique still maintains the good autocorrelation properties of the original one-dimensional sequence. In the case of the primitive root sequence, the two-dimensional autocorrelation will be two-valued and the power spectrum is flat, expect for a decrease at zero-frequency.

6.7 Diffusers

The sequences with good autocorrelation properties were turned into wall corrugations by Schroeder. When sound encounters a phase grating diffuser (see Fig. 6.10), provided that half a wavelength is larger than the width between the dividers, then plane waves will result within the wells. Plane waves propagate down each well, reflect from the bottom and return to the mouth of the diffuser. For the ith well with depth d_i, for sound with a wavelength of λ, the sound undergoes a phase change of $2jd_i(2\pi/\lambda)$ while propagating in the wells and the pressure reflection coefficient of the well at the front face of the diffuser is:

$$R_i = \exp\left(\frac{4\pi j d_i}{\lambda}\right). \tag{6.14}$$

Comparing Eqs. (6.14) and (6.11) shows that when:

$$\frac{2d_i}{\lambda} = \frac{a_i}{N}. \tag{6.15}$$

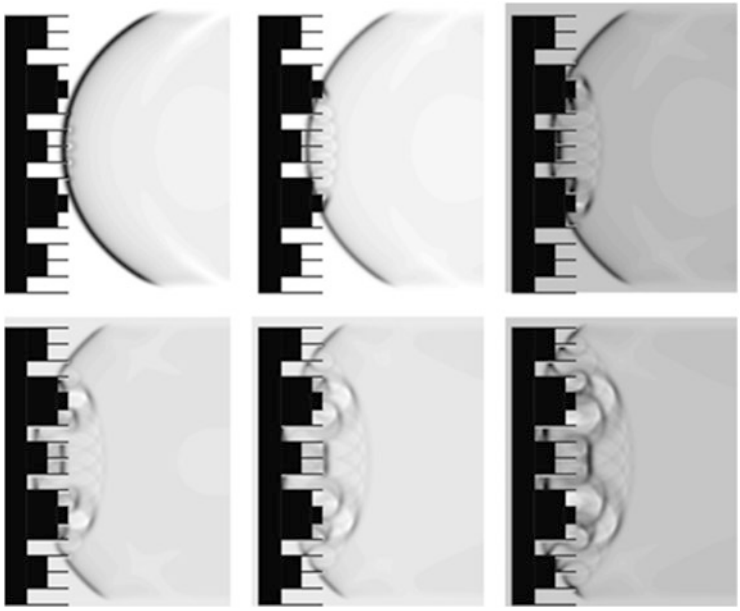

Fig. 6.10 Cylindrical wave reflected from a Schroeder diffuser calculated using a Finite Difference Time Domain (FDTD) model (after Cox and D'Antonio [6])

The sequence of sound waves reflected from the diffuser surface has the same astounding Fourier property that Schroeder identified. A rearranged version of Eq. (6.15) is therefore used to turn the number sequences into physical depths for a particular design wavelength.

What is heard some distance from the diffuser is a complicated interference pattern caused by the waves that emerged from each well before propagating to the listener. It is well-known from classical optics, that a Fourier transform of a wavefront passing through an aperture gives the far field diffraction pattern. Translating this rule for acoustic diffusers, it can be shown that the Fourier transform of the surface reflection coefficients gives the sound distribution in the far field. When there are many diffusers stacked side-by-side, the spatial periodicity causes energy to be preferentially reflected in certain directions creating so-called grating lobes. When a diffuser is formed from a quadratic residue sequence, at the design frequency these grating lobes all have the same energy. (See Fig. 9.11 in Chap. 9) This happens because the autocorrelation of the reflection coefficients is ideal.

In the 40 years since Schroeder pioneered modern diffusers for performance spaces, designs have been refined and improved as detailed in [6]. The autocorrelation of a quadratic residue sequence might be ideal at most multiples of the design frequency, but when translated into a real diffuser operating over many octaves, there are weaknesses in performance that allow room for further improvement. Researchers tried new number sequences, sequences were used in combination to

remove periodicity and fractal constructions were developed. All these designs are still, however, recognizable descendants of Schroeder's original diffusers.

One of the most ingenious features of Schroeder's work was the concept of using wells to create a set of known surface reflection coefficients. But this locked diffusers into a geometry that gave an appearance that was not liked by all architects. This drove researchers to come up with new shapes, like curves, designed using numerical optimization. While numerical optimization allows diffusers to be designed with a visual appearance to better match an architect's concept, the design method lacks the elegant simplicity of Schroeder's original ideas. Despite the complex underpinning of Schroeder's designs with number theory, the end design process was just a case of applying a few simple equations on a calculator.

References

1. Schroeder, M.R.: Improved quasi-stereophony and "Colorless" artificial reverberation. J. Acoust. Soc. Am. **33**, 1061–1064 (1961)
2. Schroeder, M.R.: Colorless artificial reverberation. J. Audio Eng. Soc. **9**, 192–197 (1961)
3. Schroeder, M.R.: Diffuse sound reflection by maximum-length sequences. J. Acoust. Soc. Am. **57**, 149–150 (1975)
4. Schroeder, M.R.: Integrated-impulse method measuring sound decay without using impulses. J. Acoust. Soc. Am. **66**, 497–500 (1979)
5. Schroeder, M.R.: Binaural dissimilarity and optimum ceilings for concert halls: more lateral sound diffusion. J. Acoust. Soc. Am. **65**, 958–963 (1979)
6. Cox, T.J., D'Antonio, P.: Acoustic Absorbers and Diffusers, 2nd edn. Taylor & Francis, London (2009)
7. Schroeder, M.R.: Number Theory in Science and Communication. Springer, Berlin (1991). 2nd enl. edn
8. Xiang, N.: Digital sequences. In: Havelock, D., Kuwano, S., Vorländer, M., et al. (eds.) Handbook of Signal Processing in Acoustics, pp. 87–106. Springer, Berlin (2008)
9. Xiang, N., Genuit, K.: Characteristic maximum-length sequences for the interleaved sampling method. Acustica **82**, 905–907 (1996)
10. Xiang, N., Schroeder, M.R.: Reciprocal maximum-length sequence pairs for acoustical dual source measurements. J. Acoust. Soc. Am. **113**, 2754–2761 (2003)
11. Xiang, N., Daigle, J.N., Kleiner, M.: Simultaneous acoustic channel measurement via maximal-length-related sequences. J. Acoust. Soc. Am. **117**, 1889–1894 (2005)
12. Ziemann, A., Arnold, K., Raabe, A.: Acoustic tomography as a method to identify small-scale land surface characteristics. Acta Acust. Acust. **87**, 731–737 (2001)
13. Xiang, N., Li, S.: A pseudo-inverse algorithm for simultaneous measurements using multiple acoustical sources (L). J. Acoust. Soc. Am. **121**, 1299–1302 (2007)
14. Gardner, W.C.: Reverberation Algorithms. Kluwer Academic Publishers, Dordrecht (1998)
15. Blesser, B.: An interdisciplinary synthesis of reverberation viewpoints. J. Audio Eng. Soc. **49**, 867–903 (2001)
16. Moorer, J.: About this reverberation business. Comput. Music J. **3**, 13–28 (1979)
17. Gardner, W.G.: Efficient convolution without input-output delay. J. Audio Eng. Soc. **43**, 127–136 (1995)
18. Van Maercke, D., Martin, J., Vian, J.-P.: Binaural simulation of concert halls: a new approach for the binaural reverberation process. J. Acoust. Soc. Am. **94**, 3255–3264 (1993)

19. Olson, S.: Understanding the perception of double-sloped energy decays: a multidimensional scaling approach. M.S. thesis, School of Architecture, Rensselaer Polytechnic Institute (2008)
20. Blauert, J.: Spatial Hearing. MIT Press, Cambridge, MA (2001)
21. Trivedi, U., Dieckman, E., Xiang, N.: Reciprocal maximum-length and related sequences for artificial spatial enveloping reverberation (A). J. Acoust. Soc. Am. **125**, 2735 (2009)
22. Trivedi, U., Xiang, N.: Utilizing reciprocal maximum length sequences within a multichannel context to generate a natural, spatial sounding reverberation (A). J. Acoust. Soc. Am. **126**, 2155 (2009)
23. Xie, B.-S., Shi, B., Xiang, N.: Audio signal decorrelation based on reciprocal maximal-length sequence filters and its applications to spatial sound. Preprint 8805, the 133rd convention of the Audio Eng. Soc., San Francisco, CA, 2012
24. Kendall, G.S.: The decorrelation of audio signals and its impact on spatial imagery. Comput. Music J. **19**, 71 (1995)
25. Daigle, J.N., Xiang, N.: A specialized cross-correlation algorithm for acoustical measurements using coded sequences. J. Acoust. Soc. Am. **119**, 330 (2006)
26. Beranek, L.: Concert Hall and Opera Houses, 2nd edn. Springer, New York (2004)
27. Schroeder, M.R.: Chaos, Power Laws: Minutes from an Infinite Paradise. W.H. Freeman & Co., San Francisco, CA (1991)
28. Fan, P., Darnell, M.: Sequence Design for Communications Applications. Wiley, New York (1996)

***

Biography

Prof. Ning Xiang earned his Ph.D. in 1990 from the Department of Electrical Engineering at the Ruhr-University Bochum (RUB) in Bochum, Germany. Since Aug 2003 he has been with the Department of Electrical, Computer, and Systems Engineering and the School of Architecture, Rensselaer Polytechnic Institute, Troy, New York, USA. Since 2005, Dr. Xiang has been the chair of the Graduate Program in Architectural Acoustics. Dr. Xiang is a Fellow of the Acoustical Society of America, a Fellow of the Institute of Acoustics (United Kingdom), and a Member of the German Acoustical Society since 1991, a Member of the Audio Engineering Society, a Member of INCE-USA, the Institute of Noise Control Engineering-USA. Dr. Xiang is currently an Associate Editor of the *Journal of the Acoustical Society of America* for the section Architectural Acoustics. In the Acoustical Society of America, he is now serving the Technical Committee Chair on Signal Processing in Acoustics. He is a recipient of Wallace Clement Sabine Medal from the Acoustical Society of America in 2014.

Prof. Bosun Xie received a Bachelor of Science degree in physics and a Master of Science degree in acoustics at South China University of Technology. In 1998, he received a Doctor of Science degree in acoustics at Tongji University. Since 1982, he has been working at South China University of Technology and is currently a professor at Acoustic Lab., School of Science. His research fields include binaural hearing, spatial sound, and sound signal processing. He has published a book named "head-related transfer function and virtual auditory display" and over 150 papers in these fields (most in Chinese). He is a vice-chairman of China Audio Engineering Society and a committee member of Acoustical Society of China.

Trevor Cox is Professor of Acoustic Engineering at the University of Salford, UK, a former Senior Media Fellow funded by the Engineering and Physical Sciences Research Council, and a past president of the UK's Institute of Acoustics (IOA). One major strand of his research is room acoustics for intelligible speech and quality music production and reproduction. Trevor's diffuser designs can be found in rooms around the world. He has co-authored a research book entitled "acoustic absorbers and diffusers." He was awarded the IOA's Tyndall Medal in 2004. Trevor has a long track record of communicating acoustic engineering to the public and has been involved in engagement projects worth over £1M. He was given the IOA award for promoting acoustics to the public in 2009. He has developed and presented science shows to 15,000 pupils including performing at the Royal Albert Hall, Purcell Rooms, and the Royal Institution. Trevor has presented 18 documentaries for BBC radio including: Life's soundtrack, Save our Sounds and Science vs. the Strad. He authored The Sound Book for W.W. Norton (entitled Sonic Wonderlands in the UK).